Development of a Takeoff Performance Monitoring System

R. Srivatsan* and David R. Downing†
University of Kansas, Lawrence, Kansas
and
Wayne H. Bryant‡
NASA Langley Research Center, Hampton, Virginia

This paper discusses the development and testing of a real-time Takeoff Performance Monitoring System. The algorithm is made up of two segments: a pretakeoff segment and a real-time segment. One-time inputs of ambient conditions and airplane configuration information are used in the pretakeoff segment to generate scheduled performance data for that takeoff. The real-time segment uses the scheduled performance data generated in the pretakeoff segment, runway length data, and measured parameters to monitor the performance of the airplane throughout the takeoff roll. Airplane and engine performance deficiencies are detected and annunciated. An important feature of this algorithm is the one-time estimation of the runway rolling friction coefficient. The algorithm was tested using a six-degree-of-freedom airplane model in a computer simulation. The results from a series of sensitivity analyses are also included.

Nomenclature

a	= acceleration (ft/s^2)
A_0, A_1, A_2, A_3	= coefficients of the acceleration cubic in true airspeed
C_D	= drag coefficient
C_L	= lift coefficient
D	= drag force (lb)
D_{RWY}	= distance along the runway (ft)
EPR	= engine pressure ratio
F	= force along an axis (lb)
g	= gravitational acceleration (ft/s^2)
H	= rate of change of height (ft/s)
I_{YY}	= y-axis moment of inertia (slug-ft^2)
L	= lift force (lb)
L_G	= landing gear force or moment (lb or ft-lb)
m	= airplane mass (slugs)
M	= pitching moment (ft-lb)
$MACH$	= Mach number
p	= roll rate (rad/s)
q	= pitch rate (rad/s)
r	= yaw rate (rad/s)
S	= reference (wing) area (ft^2)
T_0, T_1, T_2, T_3	= coefficients of the thrust cubic in true airspeed
$Temp$	= temperature (°F or °R)
THR	= engine thrust (lb)
u	= linear speed in the x direction
$\boldsymbol{u}$	= control input vector
v	= linear speed in the y direction (ft/s)
v_G	= ground speed (ft/s)
v_T	= true airspeed (ft/s)
w	= linear speed in the z direction (ft/s)
W	= airplane weight (lb)
x	= any appropriate variable
$\boldsymbol{x}$	= state vector
Γ	= discrete control effectiveness matrix
δ_{th}	= throttle position (deg)
ΔC_D	= incremental drag coefficient
ΔC_L	= incremental lift coefficient
ΔT	= iteration time step (s)
$\Delta\mu$	= incremental friction coefficient
θ_B	= pitch attitude (rad)
μ	= runway rolling friction coefficient
ξ	= discrete transform multiplier
ρ	= air density (slug/ft^3)
Φ	= discrete state matrix

Superscipts

	= time derivative
	= estimated quantity

Subscripts

B	= body axes
brake	= due to braking
C	= command
FSP	= due to flight spoilers
GSP	= due to ground spoilers
M	= measured value
n	= nth step
$n+1$	= $n+1$th step
RWY	= runway
total	= total force/moment
X_B	= along body x axis
Z_B	= along z axis

Presented as Paper 86-2145 at the AIAA Guidance, Navigation and Control Conference, Williamsburg, VA, Aug. 18-20, 1986; received Sept. 26, 1986; revision received Jan. 12, 1987.

*Aerospace Research Engineer. Member AIAA.
†Professor Aerospace Engineering. Associate Fellow AIAA.
‡Head, Systems Architecture Branch. Senior Member AIAA.

Introduction

WHILE the percentage of initiated takeoffs that have resulted in accidents is very small, accidents in this flight phase account for about 12% of all aircraft-related accidents.[1] Also, while the accident rates in all other flight phases has been decreasing in recent years, those in the takeoff phase have remained almost constant.[1]

The concept of takeoff performance monitoring is nothing new. This phase of flight has been of concern since the beginning of regulated aviation operation. Several single-point performance checks have been proposed,[2] as well as some that deal with checking the time required to attain a prespecified speed.[1]

The takeoff performance monitoring system described in this paper has the following features:

1) The system is carried on the airplane and hence is airport-independent.

2) The system detects performance deficiencies by comparing the airplane's present performance with a nominal performance for the given conditions.

3) The system computes the runway used and hence the runway available for further action.

4) The system also predicts the runway required to achieve rotation speed or to bring the airplane to a complete halt.

5) The system can be configured to operate in a fully automated mode.

This is accomplished by dividing the algorithm into two distinct segments. The first segment is used to generate nominal performance data for each takeoff. The second segment comes into play during the actual takeoff roll (real time) to check the actual performance of the airplane against the nominal performance data generated in the first segment.

Figure 1 shows a possible format for conveying the information generated by the algorithm to the flight crew. The shaded area at the top of the runway (between the total runway and the runway for achieving probation) could be used as the GO/ABORT flag with appropriate colors.

The Algorithm

At any point during the takeoff roll, the amount of runway required to achieve rotation speed is a function of the instantaneous speed of the airplane and how well it will accelerate until rotation speed. The instantaneous acceleration of the airplane is given by

$$a=\frac{THR-D-\mu(W-L)}{m} \tag{1}$$

The thrust in Eq. (1) is a function of airspeed and not easily estimated onboard an airplane. The drag and lift vary as the square of the airspeed. The rolling friction coefficient, which depends on the runway and tire conditions, is a major source of uncertainty. The airplane acceleration is seen to represent a composite measure of the performance of the airplane. A comparison of the instantaneous acceleration with a nominal value for the present airspeed is used to detect performance deficiencies.

The algorithm presented here attempts to circumvent the difficulties associated with thrust and rolling friction coefficient estimation. It consists of two segments: a pretakeoff segment and a real-time segment. For each takeoff, the pretakeoff segment is utilized to generate nominal performance data particular to that takeoff run. The real-time segment keeps track of the runway used, the runway remaining, the runway needed to achieve rotation speed, and the runway needed to bring the airplane to a complete stop. These lengths and a comparison of the actual airplane performance with the nominal value from the pretakeoff segment is used to augment the GO/ABORT decision.

The Pretakeoff Segment

The airplane acceleration performance is predicted for two extreme values of rolling friction coefficients: a low value ($\mu-0.005$) and a high value ($\mu=0.040$), using the inputs shown in Table 1. The algorithm consists of three parts as shown in Fig. 2 and can be run off-line on the onboard computers or on ground support computers with the results downloaded to the airplane computers.

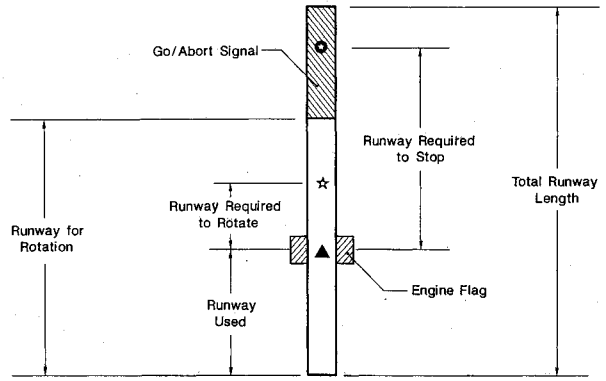

Fig 1 A typical display format for the Takeoff Performance Monitoring System.

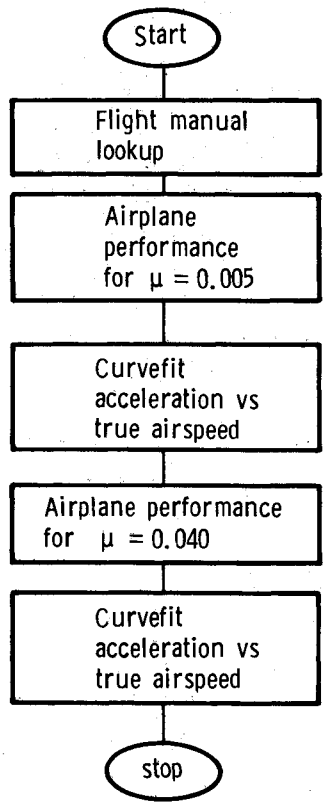

Fig. 2 Block diagram of the pretakeoff segment.

Table 1 Inputs for the pretakeoff segment

Ambient conditions	Loading and configuration information
Pressure altitude	Airplane weight
Ambient temperature	Center of gravity location
	Selected flap setting

Table 2 Flight conditions for the pretakeoff computations of Fig. 3

Weight	88504 lb
Center of gravity	19% $\bar{c}$ behind LEMAC*
Flap setting	5 deg
Presssure altitude	32 ft
Ambient temperature	75 deg °F

*where LEMAC = leading edge of mean aerodynamic chord

The first part performs a flight manual lookup to determine the recommended engine pressure ratio for takeoff, the decision speed, and the rotation speed. The throttle setting needed to achieve the engine pressure ratio is also computed.

The second part of this segment computes the airplane's scheduled acceleration performance as follows.[3-5] First the aerodynamic coefficients are extracted from the aerodynamic data base for the airplane as a function of the motion variables. The aerodynamic forces and moments are computed in the airplane stability axis system. These forces and moments are then transformed into the body axis system. The components of the engine forces and moments along the body axes are determined using the manufacturer-supplied engine model. A manufacturer-supplied landing gear model is utilized in computing the landing gear forces and moments along the body axis system.

The primary contribution to the longitudinal acceleration comes from the force along the body x axis and is obtained as

$$F_{X_{B_{\text{Total}}}} = F_{X_B} + THR_{X_B} + L_{G_{XB}} \tag{2}$$

and the acceleration component resulting from this and the runway slope are computed using

$$\dot{u}_B = (F_{X_{B_{\text{Total}}}}/m) - g\sin\theta_B \tag{3}$$

Although the minor contributions from pitching and other rotational products are included in the pretakeoff segment, they are not shown here. In the preceding computations, a nominal throttle movement time history was chosen to duplicate typical operational procedures. This throttle position serves as the input to a throttle servo with the following dynamics:

$$\delta_{\text{th}}(n\Delta T) = \xi\delta_{\text{th}}[(n-1)\Delta T] + (1-\xi)\delta_{\text{th}_C}(n\Delta T) \tag{4}$$

The last part of this segment deals with curve fitting along the acceleration track a as a function of the airplane true airspeed v_T to generate a set of coefficients for a "nominal performance" data set for the takeoff run. A least-square-error cubic polynomial curvefit method[6] is utilized to generate

$$a = A_0 + A_1 v_T + A_2 v_T^2 + A_3 v_T^3 \tag{5}$$

This process is carried out twice, once for the low-friction coefficient and a second time for the high-friction coefficient. Figure 3 illustrates the results obtained from the pretakeoff segment for the takeoff conditions of Table 2.

The Real-Time Segment

A block diagram of the real-time segment is shown in Fig. 4. This segment performs the following functions:

1) It initially commands the throttle to the required throttle setting for takeoff.

2) It monitors the engine in terms of its engine pressure ratio.

3) It monitors the performance of the airplane in terms of its acceleration performance.

4) It estimates the runway rolling friction coefficient.

5) It predicts the runway required to achieve rotation speed.

6) It predicts the runway required to stop the airplane and generates go or abort signals.

The real-time segment requires several input parameters. Some of these are one-time inputs while others are continuously needed inputs. Table 3 lists all of these input parameters. The pressure altitude and ambient temperature inputs are used to compute the air density and temperature and pressure ratios (atmospheric calculations) once during the real-time segment.

The generation of a basis for scheduled performance consists of interpolating between the sets of coefficients generated in the pretakeoff segment [Eq. (10)] to obtain a set of coeffi-

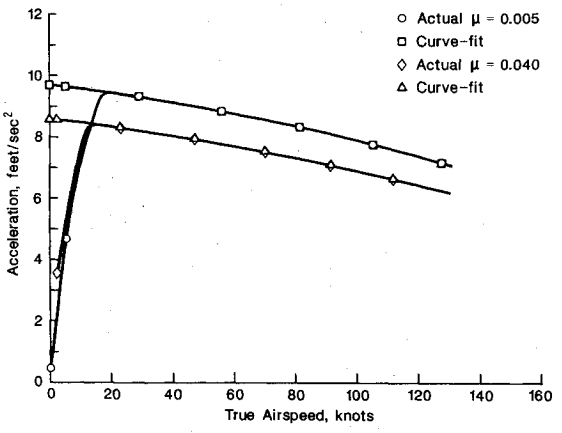

Fig. 3 Acceleration time histories and their curvefit from the pretakeoff segment.

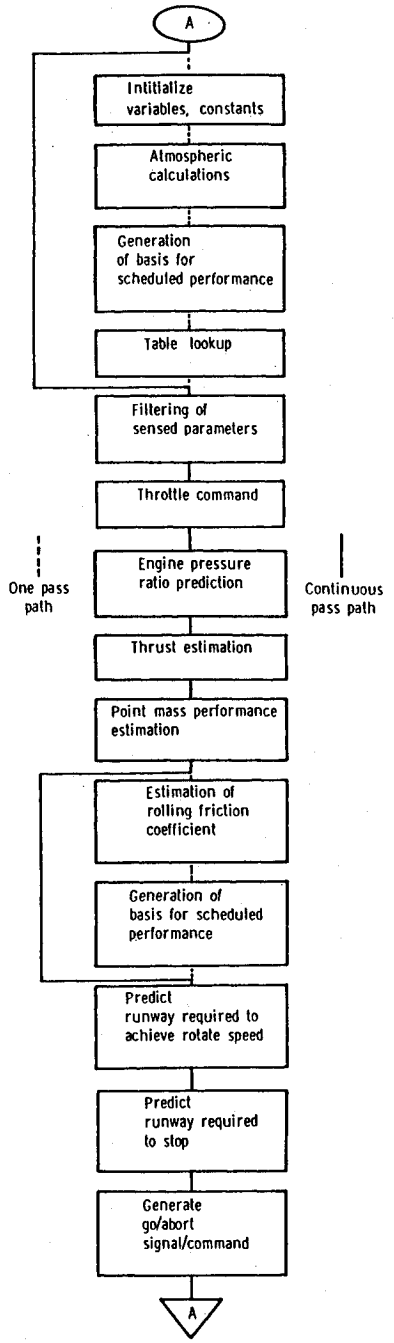

Fig. 4 Block diagram of the real-time segment.

cients corresponding to the input value for nominal rolling friction coefficient (Table 3). This one-time computation gives an initial basis for performance comparisons.

Two table lookups are performed in this segment. The first lookup obtains the flight manual-recommended stabilizer setting for the given airplane loading configuration. The nominal lift and drag coefficients for the present takeoff roll, increments in the lift and drag coefficients with full deflection of the flight, and ground spoilers are also determined. The other lookup function is identical to the one in the pretakeoff segment.

Values for the continuously needed parameters are supplied by sensors on the airplane. Before use by the system, these sensor outputs are processed through a filter implementation. The measured acceleration and ground speed are processed through a second-order complementary filter to estimate the bias present in the acceleration signal as follows:[3,7]

$$x_{n+1} = \Phi x_n + u_n \tag{6a}$$

where

$$x = \begin{bmatrix} x(1) \\ x(2) \end{bmatrix}$$

$$u = \begin{bmatrix} v_G \\ a_M \end{bmatrix}$$

$$\hat{v}_G = x(1) \tag{6b}$$

$$a_{F1} = a_M + x(2) \tag{6c}$$

The acceleration output from the complementary filter (a_{F1}) measured values of the engine pressure ratio (left and right), and calibrated airspeed are passed through a first-order lag filter[3,8] to remove noise, and the outputs from this filter are the values used by the system. The throttle command block generates a throttle movement history identical to the one used in the pretakeoff segment.

An empirical model of the steady-state behavior of the engine pressure ratio and thrust is extracted from the manufacturer-supplied engine model to predict these parameters as follows:

$$\hat{EPR}_{\substack{\text{left} \\ \text{right}}} = f(\delta_{\text{th}_{\substack{\text{left} \\ \text{right}}}}, \text{Temp}_{\text{total}}) \tag{7}$$

$$\hat{THR}_{\text{left}} = f(EPR_{\substack{\text{left} \\ \text{right}}}, MACH) \tag{8}$$

A point mass formulation of the equations of motion is used to estimate the performance of the airplane.[3,9] First the wind speed and measured ground speed are combined to obtain the true airspeed, Mach number, and dynamic pressure. The nominal lift and drag coefficients yield the lift and drag forces. Combining these with the weight and rolling friction coefficient (input value) and the estimated thrust (based on the measured engine pressure ratio) results in an estimated airplane acceleration. The measured ground speed is numerically integrated (rectangular integration) to obtain the distance along the runway.

One salient feature of this algorithm is the estimation of the runway friction coefficient in real time. This is a single-point estimate carried out a few seconds (10 s in this implementation) into the takeoff run. The estimation takes place as follows. First the thrust is represented as a cubic in airspeed:

$$THR = T_0 + T_1 v_T + T_2 v_T^2 + T_3 v_T^3 \tag{9}$$

Substituting this and the expressions for lift and drag in terms of the aerodynamic coefficient into Eq. (1) along with an assumed friction coefficient, the estimated acceleration is obtained as

$$\hat{a} = g[(T_0 - \hat{\mu}_1 W) + T_1 v_T + (T_2 - \tfrac{1}{2}\rho S C_D + \tfrac{1}{2}\hat{\mu}_1 \rho S C_L) v_T^2 + T_3 v_T^3]/W \tag{10a}$$

Writing a similar expression for the actual acceleration in terms of an estimate of the actual friction coefficient ($\hat{\mu}_2$) at the same true airspeed (v_T),

$$a = g[(T_0 - \hat{\mu}_2 W) + T_1 v_T + (T_2 - \tfrac{1}{2}\rho S C_D + \tfrac{1}{2}\hat{\mu}_2 \rho S C_L) v_T^2 + T_3 v_T^3]/W \tag{10b}$$

Subtracting the second equation from the first and rearranging to obtain the difference between the two friction coefficients (since all other parameters are known),

$$\Delta\hat{\mu} = \hat{\mu}_2 - \hat{\mu}_1 = (\hat{a} - a)/[g(W - \tfrac{1}{2}\rho S C_L v_T^2)/W] \tag{11}$$

where

$\hat{\mu}_2$ = estimate of the actual runway friction coefficient (unknown)
$\hat{\mu}_1$ = assumed friction coefficient (known)
$\Delta\hat{\mu}$ = estimated difference in the friction coefficients (computed)

Thus, the actual rolling friction coefficient is estimated as

$$\hat{\mu}_2 = \hat{\mu}_1 + \Delta\hat{\mu} \tag{12}$$

Immediately after this process, the basis for scheduled performance is recomputed with $\hat{\mu}_2$ as the present estimate of the friction coefficient.

The runway required to achieve rotation speed is computed by a 10 step rectangular integration scheme between the present true airspeed and the true airspeed for rotation. The acceleration in each interval is assumed to remain constant at a value given by the scheduled performance basis for the true airspeed at the midpoint of the interval.

Table 3 Parameters needed for the real-time segment

One-time inputs		Needed continuously
Ambient temperature		Left and right throttle position
Ambient pressure		Left and right engine pressure ratio
Runway wind	Obtained from the pretakeoff segment	Ground speed
Weight		Along track acceleration
Flap setting		Calibration airspeed
Stabilizer setting		
Runway available for rotation		
Runway available for stopping		
Nominal rolling friction coefficient		

Table 4 Sensor noise and bias characteristics

All noises are Gaussian with standard deviations as indicated.

Parameter	Sigma (standard deviation)	Bias (constant bias value)
Along track acceleration	0.32	0.32
Calibration airspeed (kts)	2.0	0.0
Throttle position (deg)	0.2	−0.4
Engine pressure ratio	0.01	0.02

To calculate the stopping distance, the system simulates the effect of a series of commands to deploy the flight and ground spoilers, to reduce the throttle to an idle setting, and to apply full braking. The computations are based on the following assumptions:

1) The flight and ground spoilers are commanded through servos modeled as first-order lags.

2) With full braking, the rolling friction coefficient is increased by a constant amount over the prevalent value.

3) Maximum wheel braking is achieved in a ramp fashion per given time period.

4) Thrust is assumed to vary linearly from the present value to idle thrust with throttle position (reaching idle thrust for a throttle position of zero).

5) Changes in the lift and drag coefficients produced by flight and ground spoilers are assumed to vary linearly with deflection.

Using these assumptions in a numerical integration scheme based on incremental time, the stopping distance is computed in a point mass formulation with the lift and drag coefficients computed as

$$C_L = C_{L_{\text{nominal}}} + \Delta C_{L_{FSP}} + \Delta C_{L_{GSP}} \tag{13}$$

$$C_D = C_{D_{\text{nominal}}} + \Delta C_{D_{FSP}} + \Delta C_{D_{GSP}} \tag{14}$$

and the friction coefficient as

$$\mu = \mu_{\text{nominal}} + \Delta\mu_{\text{brake}} \tag{15}$$

Generation of GO/ABORT Signal

The engine pressure ratio is used as a check on engine health. After allowing time for the engine transients to die out, the measured value is compared with the predicted value (corresponding to the measured throttle position). If this difference is more than a preselected limit, an engine failure flag is set:

$$\frac{EPR_{1/r} - \hat{EPR}_{1/r}}{EPR_{1/r}} > EPR_{\text{error limit}} \Rightarrow \text{Engine failure}_{1/r} \tag{16}$$

At any time after the rolling friction coefficient is estimated, any difference between the measured and the predicted accelerations exceeding a preselected limit causes a performance failure flag to be set:

$$\frac{a - \hat{a}}{a} > a_{\text{error limit}} \Rightarrow \text{Performance failure} \tag{17}$$

With these flags, the following conditions result in a Go signal:

1) No engine failure flag or performance failure flag is set, and the runway length available is greater than the runway length required to achieve rotation speed.

2) Only one engine failure flag is set, and the runway remaining is less than that required for stopping the airplane.

3) The performance failure flag is set without either engine failure flag being set, and there is insufficient runway length for stopping.

The following conditions result in an Abort signal:

1) The runway length available for achieving rotation speed is less than that required.

2) Both engine failure flags are set.

3) One engine failure flag is set, and there is sufficient runway length available for stopping.

4) The performance failure flag is set, and sufficient runway length is available for stopping.

Table 5 Normal takeoff test cases

Case	Pressure altitude (ft)	Temperature (°F)	Runway wind (knots)	Weight (lb)	Friction coefficient
I	32	75	0	88,504	0.015
II	0	75	0	88,504	0.015
III	100	75	0	88,504	0.015
IV	32	0	0	88,504	0.015
V	32	100	0	88,504	0.015
VI	32	75	10	88,504	0.015
VII	32	75	20	88,504	0.015
VIII	32	75	0	88,504	0.025
IX	32	75	0	88,504	0.007
X	32	75	0	98,000	0.015

Table 6 Summary of results for cases in Table 5

Case	Measured case @ rotation	Runway used	Runway prediction error	Updated friction coefficient
I	128.1	3,262	−130	0.017
II	128.3	3,266	−142	0.017
III	128.6	3,277	−128	0.017
IV	129.1	2,740	−58	0.017
V	129.4	3,603	+22	0.018
VI	129.1	2,685	+5	0.017
VII	128.8	2,300	−11	0.018
VIII	128.2	3,272	−26	0.027
IX	128.1	3,085	−40	0.009
X	138.1	4,155	−13	0.017

Testing

The algorithm described in the previous sections was specialized for a typical twin-jet airplane and evaluated using a six-degree-of-freedom batch simulation model running at 20 times a second. The simulation utilizes a pseduo-random number generator to superimpose zero mean Gaussian noise signals with any chosen standard deviations on any of the sensed parameters. Table 4 lists the sensed parameters used for this checkout along with their corresponding standard deviations and biases.

The pretakeoff computations use an iteration time step of 0.05 s. The computations of this segment are carried out prior to the start of the batch simulation.

The takeoff performance monitoring system is called 10 times a second, or every other iteration cycle from the batch simulation. Some of the parameters used in this segment are as follows:

$$\Delta T = 0.1 \text{ s}$$

$$\Delta\mu_{\text{brake}_{\max}} = 0.45$$

$$t_{\text{ramp}_{\text{brake}}} = 0.6 \text{ s}$$

$$EPR_{\text{error limit}} = 0.15$$

$$a_{\text{error limit}} = 0.15$$

Normal Takeoff Test Cases

Ten cases are presented to demonstrate the normal performance of the algorithm. These cases, listed in Table 5, represent different combinations of loading and ambient conditions. An actual airplane under these conditions would have gone through a successful ground roll and rotation. Table 6 summarizes the results obtained for the cases listed in Table 5. The second column shows the measured calibrated airspeed at rotation (more precisely, the instant at which the simulation

Table 7 Effect of wind speed error

Wind speed			Performance	
Assumed (knots)	Actual (knots)	Adjusted (μ)	Runway prediction error (ft)	Δ prediction error (ft)
10	0	0.012	−615	−620
10	10	0.017	5	0[a]
10	20	0.022	447	442
20	0	0.007	−1,058	−1,046
20	10	0.012	−144	−432
20	20	0.017	−12	0[a]
20	30	0.023	428	440

[a]Nominal case.

Table 8 Effect of ambient temperature error

Temperature			Performance	
Assumed (°F)	Actual (°F)	Adjusted (μ)	Runway prediction error (ft)	Δ prediction error (ft)
50	25	0.017	347	348
50	50	0.017	−40	0[a]
50	75	0.017	−505	−465

[a]Nominal case.

Table 9 Effect of gross weight errors

Weight			Performance	
Assumed (lb)	Actual (lb)	Adjusted (μ)	Runway prediction error (ft)	Δ prediction error (ft)
88,504	78,504	−0.021	−55	75
88,504	88,504	0.017	−130	0[a]
88,504	98,504	0.048	61	191

[a]Nominal case.

Table 10 Effect of flap setting errors

Flap setting			Performance	
Assumed (deg)	Actual (deg)	Adjusted (μ)	Runway prediction error (ft)	Δ prediction error (ft)
5	1	0.017	−155	−25
5	5	0.017	−130	0[a]
5	15	0.017	−144	−14

[a]Nominal case.

was terminated as having achieved rotation speed). The prediction error in column four of this table is the amount by which the runway requirement prediction was in error. A negative number in this column indicates that the airplane used that much more runway than was predicted by the algorithm. It is seen that this error is less than 5% of the runway used. The last column shows the updated friction coefficient after 10 s into the takeoff run. This is the algorithm-estimated friction coefficient for that takeoff run as opposed to the actual value (column six of Table 5). Figure 5 shows the time histories of the predicted runway requirements and the runway used for case I of Table 5. Also shown in this plot is the sum of the two instantaneous values. This line measures the

Table 11 Effects of aerodynamic degradation

Degradation		Performance	
Level	Adjusted (μ)	Runway prediction error (ft)	Δ Prediction error (ft)
0	0.017	−130	0[a]
10%	0.018	−140	−10
15%	0.018	−156	−26

[a]Nominal case.

Table 12 Effects of reduced calls to the algorithm

		Performance	
Frequency of calls	Adjusted (μ)	Runway prediction error	Δ Prediction error
10	0.017	−130	0[a]
5	0.002	−205	−75

[a]Nominal case.

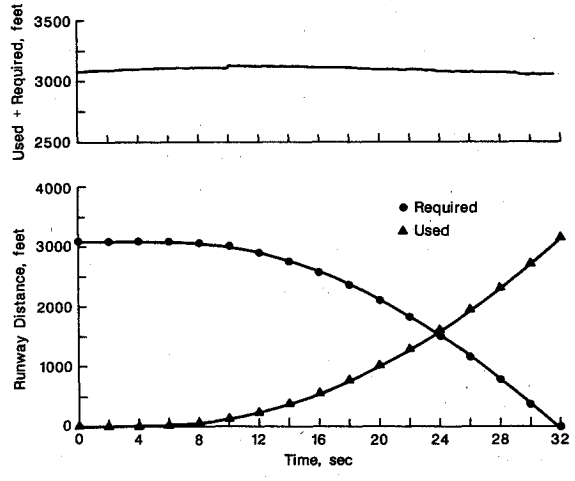

Fig. 5 Plots of runway required and used for Case I and Table 5.

"goodness" of the algorithm prediction. For a good runway length predictor, this line should remain a horizontal straight line, i.e., at any given instant the predicted runway required to achieve rotation speed is equal to the prediction at any previous time minus the runway used between the two points. The downward shift in the runway required curve and the consequent shift in the sum is caused by the estimation of the friction coefficient at 10 s.

Engine Malfunction Test Cases

Two types of engine malfunctions are simulated for this study: 1) the engine does not develop handbook EPRs, and 2) the engine does not develop handbook thrust. For the first case, the EPRs in the simulation are forced to 15% above and below their nominal values. For both the above- and below-nominal EPR cases, an engine failure flag was set at the 10-s mark.

Engine thrust malfunction is simulated by forcing the thrust to 15% above and below the nominal value. It is assumed that the thrust degradation does not affect the EPRs. The EPR output from the engine still corresponds to the nominal value. Since the EPR is the only parameter used for the engine health check, neither case results in an engine failure flag. At the 10-s point the difference between the measured and predicted accelerations is attributed to a faulty friction coefficient input.

For the 115% thrust case, this results in an updated friction coefficient of −0.028 (changed from 0.015), and for the 85% thrust case, the dated friction coefficient is 0.063. These values are well out of the nominal range of 0.015–0.040.

Sensitivity and Failure Mode Analysis

The sensitivity of the algorithm to input errors and the effects of sensor failures are considered here. The sensitivity analysis is carried out by forcing selected inputs to the algorithm and the simulation to be different and comparing the algorithm's predictions with the true values generated by the simulation. The failure analysis is carried out by causing the sensor outputs from the simulation model to be in error and again comparing the predictions with performance. Case I of Table 5 serves as the baseline for all of the analyses of this section. In addition, the baseline flap setting is 5 deg.

Sensitivity to Errors in Inputs

The first parameter considered is runway winds. The algorithm and the simulation are forced to use different runway wind conditions. The results are summarized in Table 7. It is seen that the algorithm is highly sensitive to errors in runway winds. No abort signal is generated by the algorithm. At the 10-s point, the difference between the predicted and measured acceleration is used to generate a friction coefficient value that in several cases is quite different from the actual value. An onboard wind estimator is considered in an effort to reduce this sensitivity. The runway winds are estimated as being the difference between the measured and algorithm-computed/calibrated airspeed prior to estimating the friction coefficient, as a one-time operation. The prediction error changed from 1,058 ft without a wind estimator to −139 ft (with an assumed head wind of 20 knots vs an actual no-wind condition).

It is seen from Table 8 that the algorithm is sensitive to errors in ambient temperature inputs. Even though the estimated friction coefficient is not appreciably different from the actual value, the error in the runway requirements increased to about 10% of the total used.

The effect of errors in the gross weight input are summarized in Table 9. Even though the error in the predicted runway requirements is rather small, the adjusted friction coefficient is seen to be very much different from the actual value of 0.015. The difference between the measured and predicted accelerations caused by the weight error is treated as being caused by a friction coefficient discrepancy at the 10-s mark. The other problem with this situation is that the airplane rotation speed is based on the 88,504-lb weight and thus results in a premature rotation for the overweight case. In the underweight case, the airplane will remain on the runway longer than needed.

The effects of flap setting errors are summarized in Table 10. The runway prediction errors are seen to be small for the chosen rotation speed. But again the chosen rotation speeds are based on the wrong flap setting.

Sensitivity to Aerodynamic Degradation

Table 11 summarizes the effects of aerodynamic degradation such as that caused by ice formation on the wings. The two cases explored are a 10% reduction in lift accompanied by a 10% increase in drag and a 15% degradation. In both cases the friction coefficient is adjusted in a minor way to bring the runway length predictions very close to nominal.

The effects of the reduced frequency of calls to the takeoff performance algorithm are shown in Table 12. At five calls per second, the friction coefficient is seen to be adjusted to a rather low value. The prediction error goes to just over 5% of the total runway used.

Failure Analysis

The effects of accelerometer biases are shown in Table 13. The algorithm is seen to be able to handle accelerometer biases of at least ±2 ft/s² over the nominal value without significant changes to the friction coefficient or the runway prediction.

Table 13 Effects of accelerometer biases

	Performance		
Accelerometer bias (f/s²)	Adjusted (μ)	Runway prediction error (ft)	Δ prediction error (ft)
2.32	0.016	−150	−20
0.32	0.017	−130	0[a]
−1.68	0.017	−130	0

[a]Nominal case.

Table 14 Effects of accelerometer scaling

	Performance		
Accelerometer scale factor	Adjusted (μ)	Runway prediction error (ft)	Δ prediction error (ft)
85%	0.029	7	137
100%	0.017	−130	0[a]
115%	0.006	−253	−123

[a]Nominal case.

The effect of a 15% scaling of the accelerometer is shown in Table 14. This caused a significant change in the estimated friction coefficient. The runway prediction error is increased to just over 5% for the 115% accelerometer scaling case.

Introducing a bias of −0.3 in the engine pressure ratio measurement (16% of an EPR of 2.0 subtracted from the nominal bias of 0.02) caused an engine failure flag to be set. A bias of −0.34 also had a similar effect. Introducing a scale factor error of 15% on the engine pressure ratio measurement on either side of nominal caused engine failure flags to be set. Forcing the ground speed sensor output to 100 ft/s and 250 ft/s caused a performance failure flag to be set.

Concluding Remarks

A Takeoff Performance Monitoring System has been developed and tested using a batch simulation of the NASA TSRV B-737 airplane. Ten normal takeoff cases were used in testing the algorithm. The runway required was found to be predicted within 5% of the overall runway used.

Engine malfunctions that affected the engine pressure ratio were detected and engine failure flags were raised. Sensitivity analysis indicates that the algorithm is highly sensitive to errors in runway wind inputs. An onboard wind estimator reduces this sensitivity. The algorithm is also sensitive to errors in ambient temperature inputs. Errors in weight inputs were found to cause the runway friction coefficient to be adjusted to unreasonable values. Errors in the flap setting were accounted for by changing the friction coefficient, but the rotation speed was based on the erroneous flap setting input. Aerodynamic degradations of 10 and 15% did not cause any problems. The frequency of calls to the algorithm could not be halved (changed from the 10 calls per second to five calls per second).

The algorithm has the capability to adjust for accelerometer bias and scale factor errors. Engine pressure ratio biases of 15% of nominal and 15% scale factors caused engine failure flags to be raised. Failed ground speed sensors raised a performance failure flag. The errors associated with inputs could be eliminated for the most part by automating these inputs.

References

[1]*Minutes of the first meeting of the SAE Takeoff Performance Monitoring Ad Hoc Committee of the Aircraft Division of the Aerospace Council,* Washington, DC, May 15–16, 1984.

[2]Small, Maj. J.T., "Feasibility of Using Longitudinal Acceleration (N_x) for Monitoring Takeoff and Stopping Performance from the Cockpit," A84-16157 05-05, *Proceedings of the Twenty-Seventh Symposium,* Beverly Hills, CA, Sept. 28–Oct. 1, 1983.

[3]Srivatsan, R., *Design of a Takeoff Performance Monitoring System,* D.E. Dissertation. University of Kansas, June 1985.

[4]Etkin, B., *Dynamics of Atmospheric Flight,* Wiley, New York, 1972.

[5]Roskam, J., *Airplane Flight Dynamics and Automatic Flight Controls, Part I,* Roskam Aviation and Engineering Corp., 1979.

[6]*Mathematical and Statistical Software at Langley*, Central Computing Complex Document N-3, NASA Langley Research Center, April 1984.

[7]Pines, *Terminal Area Automatic Navigation, Guidance, and Control Research Using the Microwave Landing System (MLS): Part 2—RNAV/MLS Transition Problems for Aircraft,* NASA CR-3511, Jan. 1982.

[8]Franklin, G.F. and Powell, J.D., *Digital Control of Dynamic Systems,* Addison-Wesley, June 1981.

[9]Lan, C-T. E. and Roskam, J., *Airplane Aerodynamics and Performance,* Roskam Aviation and Engineering Corp., 1981.